ASED http://e-ASED.org
Animal Systematics, Evolution and Diversity

Anim. Syst. Evol. Divers. Vol. 34, No. 1: 37-49, January 2018
https://doi.org/10.5635/ASED.2018.34.1.024

Redescription of *Australocirrus shii* and First Report of *Afrokeronopsis aurea* (Ciliophora: Spirotrichea: Sporadotrichida) from South Korea

Ahmed Salahuddin Kabir, Daizy Bharti, Mann Kyoon Shin*

Department of Biological Sciences, College of Natural Sciences, University of Ulsan, Ulsan 44610, Korea

ABSTRACT

Two hypotrich ciliates, *Australocirrus shii* (Shi et al., 1997) Kumar & Foissner, 2015 and *Afrokeronopsis aurea* (Foissner & Stoeck, 2008) Foissner et al., 2010 isolated from freshwater habitats in Korea and were studied based on the specimens from live and after protargol impregnation. *Australocirrus shii* is redescribed based on morphology and 18S rRNA gene sequence, whereas *Af. aurea* is the first record for Korea. Main morphological features of the Korean population of *Au. shii* are as following: body size 100−200 × 40−80 μm *in vivo*; elongate to ellipsoidal or slightly elongate obovate, dorsoventrally flattened; transverse cirri arranged in (3 + 2) pattern, anterior pretransverse ventral cirrus distantly anterior of the first transverse cirrus; eight or nine dorsal kineties; and three caudal cirri. Main morphological features of the Korean population of *Af. aurea* are as following: body size 230−375 × 70−145 μm *in vivo*; shape elongate obovate or ellipsoidal, widest at the mid-body; undulating membranes in *Australocirrus* pattern with a buccal depression; and three caudal cirri. The Korean population of *A. shii* is similar in morphology with previous descriptions except for the presence of indentation at the posterior end in the Korean population. The Korean population of *A. aurea* is slightly shorter than the South African population and has slightly less marginal and mid-ventral cirri. The phylogenetic analysis of present two Korean hypotrichs and relevant species based on 18S rRNA gene sequences generated almost similar tree topologies compared with previous studies.

Keywords: morphology, 18S rRNA gene, phylogenetic analysis

INTRODUCTION

Foissner and Stoeck (2008) established the family Neokeronopsidae and included the genus *Pattersoniella* Foissner, 1987 and two subgenera, i.e., *Neokeronopsis* (*Neokeronopsis*) and *N.* (*Afrokeronopsis*) in agreement with the CEUU hypothesis (convergent evolution of a midventral cirral pattern in urostylid and oxytrichid hypotrichs) (Foissner et al., 2004). Later, Foissner et al. (2010) changed the rank of subgenus *Afrokeronopsis* to the genus level with *Af. aurea*, the type species for *Afrokeronopsis*. Kim et al. (2014), based on the molecular analyses, proposed the classification of the genus *Pattersoniella* in the family Oxytrichidae and added a novel genus, i.e., *Apoterritricha*, to the family Neokeronopsidae. Thus at present state the family Neokeronopsidae includes three genera, i.e., *Neokeronopsis*, *Afrokeronopsis*, and *Apoterritricha*. The detailed description of the type species of the genus *Afrokeronopsis*, i.e., *Af. aurea* (Foissner & Stoeck, 2008) (see Foissner et al., 2010) has been provided in the present study.

The genus *Australocirrus* was established by Blatterer and Foissner (1988) as an oxytrichid genus with the main characters of typical ventral ciliature (18 cirri), strongly fragmented dorsal kinety 3, and presence of caudal cirri based on the type species *Au. oscitans*. After then, the subgenus *Cyrtohymenides* was established by Foissner (2004) with the type species *Cyrtohymena* (*Cyrtohymenides*) *aspoecki*. Recently, Kumar and Foissner (2015) synonymized the genus *Australocirrus* Blatterer & Foissner, 1988 with the subgenus *Cyrtohymenies* Foissner, 2004 mainly based on the detailed investigation on the oral apparatus (separating undulating membranes pattern of *Australocirrus* from the *Cyrtohymena* pattern) of two cyrtohymenid species, i.e., *Au. shii* (Shi et al., 1997) and *Au. australis* (Foissner, 1995). The species of

***To whom correspondence should be addressed**
Tel: 82-52-259-2396, Fax: 82-52-259-1694
E-mail: mkshin@ulsan.ac.kr

eISSN 2234-8190

Au. shii was described inappropriately as *Au. australis* (= *Cyrtohymena australis*) in Korea due to the lack of literature at that time (Kim et al., 2012); thus, it is necessary to amend the name and improve its morphological description.

The present investigation aims to improve the morphological features and 18S rDNA phylogeny of two species of Korean hypotrichs, *Af. aurea* and *Au. shii*, and add new information on the Korean ciliate fauna.

MATERIALS AND METHODS

Sample collection and culturing

Australocirrus shii was collected from a fresh water stream near the southwest of South Korea (Songho-ri, Jisan-myeon, Jindo-gun, Jeollanam-do, South Korea, 34°24′04.8″N, 126° 08′22.9″E) on 8 Jul 2016. *Afrokeronopsis aurea* was collected from a fresh water river in the middle of Korean peninsula (Oepyeong-ri, Geumsa-myeon, Yeoju-si, Gyeonggi-do, South Korea, 37°18′13.4″N, 127°37′06.8″E) on 11 Aug 2016. The surface water (~30 cm) including sediments were collected and transported to the laboratory for further processing. Samples were then transferred to Petri dishes together with sediments and maintained at room temperature until two weeks. To promote the growth of bacteria and bacterivorous flagellates, a few wheat kernals were added to the Petri dishes (Li et al., 2010). Clonal cultures of *Au. shii* and *Af. aurea* were established by isolating single specimen from the raw culture and feeding them with the green algae *Chlorogonium elongatum* (Ammermann et al., 1974). Same culture was then used for live observation, protargol staining, and DNA isolation.

Morphological observations

Live specimens were observed under dissecting and optical microscope at magnifications ranging from 50× to 1,000×.

Table 1. Morphometric data of *Australocirrus shii* Korean population

Characters	Mean	M	SD	SE	CV	Min	Max	n
Body, length	139.6	140.5	13.4	3.0	0.1	115.0	168.0	20
Body, width	43.8	43.5	5.7	1.3	0.1	37.0	61.0	20
Body length : width, ratio	3.2	3.3	0.2	0.0	0.1	2.8	3.4	20
AZM, length	55.3	56.0	3.1	0.7	0.1	48.0	61.0	20
Body length : AZM length, ratio	2.5	2.5	0.2	0.0	0.1	2.1	2.9	20
Longest AM	9.9	10.0	1.0	0.2	0.1	8.0	13.0	20
AM, number	47.9	48.5	3.6	0.8	0.1	40.0	55.0	20
Anterior body end to anterior MA nodules, distance	45.8	46.5	3.6	0.8	0.1	38.0	54.0	20
MA nodules, distance in between	14.3	14.0	4.3	1.0	0.3	7.0	22.0	20
Anterior MA nodule, length	16.7	16.0	2.5	0.5	0.1	13.0	22.0	20
Anterior MA nodule, width	8.6	8.0	0.9	0.2	0.1	8.0	11.0	20
Posterior MA, length	19.9	20.0	2.5	0.5	0.1	16.0	27.0	20
Posterior MA, width	8.3	8.0	0.9	0.2	0.1	7.0	10.0	20
MA nodules, number	2.0	2.0	0.0	0.0	0.0	2.0	2.0	20
MI, diameter	2.9	3.0	0.5	0.1	0.9	1.0	4.0	20
MI, number	2.9	3.0	0.8	0.2	0.3	1.0	4.0	20
RMC, number	28.2	28.0	2.1	0.5	0.1	24.0	32.0	20
LMC, number	28.5	28.5	2.6	0.6	0.1	23.0	35.0	20
FC, number	3.0	3.0	0.0	0.0	0.0	3.0	3.0	20
Anterior body end to BC, distance	22.1	21.5	4.2	0.9	0.2	18.0	38.0	20
BC, number	1.0	1.0	0.0	0.0	0.0	1.0	1.0	20
FVC, number	4.1	4.0	0.2	0.1	0.1	4.0	5.0	20
PVC, number	3.0	3.0	0.0	0.0	0.0	3.0	3.0	20
TC, number	5.0	5.0	0.0	0.0	0.0	5.0	5.0	20
Anterior TC to anterior most PTC, distance	12.1	12.0	1.5	0.3	0.1	9.0	15.0	20
PTC, distance in between	15.5	15.5	1.8	0.4	0.1	12.0	19.0	20
PTC, number	2.0	2.0	0.0	0.0	0.0	2.0	2.0	20
CC, number	3.0	3.0	0.0	0.0	0.0	3.0	3.0	20
Buccal field, max width	12.6	13.0	1.7	0.4	0.1	10.0	16.0	20
DK, number	8.6	9.0	0.5	0.2	0.1	8.0	9.0	20

Data based on mounted, protargol-impregnated, and randomly selected specimens from a nonflooded Petri dish culture. Measurements of length or width or distance in μm.

Mean, arithmetic mean; M, median; SD, standard deviation; SE, standard error of arithmetic mean; CV, coefficient of variation in %; Min, minimum; Max, maximum; n, number of individuals investigated; AZM, adoral zone of membranelles; AM, adoral membranelles; BC, buccal cirrus; CC, caudal cirri; DK, dorsal kineties; FC, frontal cirrus; FVC, frontoventral cirri; LMC, left marginal cirri; MA, macronucleus; MI, micronucleus; PTC, pre transverse cirri; PVC, postoral verntral cirri; RMC, right marginal cirri; TC, transverse cirri.

Protargol staining was performed to observe ciliatures and nuclear apparatus (Wilbert, 1975; Kamra and Sapra, 1990). Drawings of living cells were based on free-hand sketches and with the help of drawing devices. The classification and terminology are basically according to Berger (1999), Foissner and Stoeck (2008), and Lynn (2008).

DNA isolation, polymerase chain reaction (PCR) amplification, and sequencing

Several cells were collected from the culture medium and subsequently washed with sterilized distilled water. Genomic DNA was extracted using the RED Extract-N-Amp Tissue PCR Kit (Sigma, St. Louis, MO, USA) according to the manufacture's protocol. PCR cycling parameters followed the protocol described in Shazib et al. (2014).

Sequence processing and alignment

All raw sequences were imported and assembled into contigs in Geneious ver. 8.1.4 generated by Biomatters (http://www.geneious.com) (Kearse et al., 2012). A total of 53 18S ribosomal RNA (18S rRNA) gene sequences, which were found to be related to the newly characterised sequences, were retrieved from the NCBI GenBank and were aligned using ClustalW alignment in Geneious. The unreliable columns were removed through editing in Gblocks version 0.91b (http://molevol.cmima.csic.es/castresana/Gblocks_server.html) (Castresana, 2000; Talavera and Castresana, 2007). The final alignment file contained 1,671 unambiguously aligned nucleotide characters. Pairwise uncorrected *p-distances* and numbers of nucleotide differences in the 18S rRNA gene sequences within all species were calculated using MEGA version 6 (Tamura et al., 2013).

Phylogenetic analyses

18S rRNA gene was used for phylogenetic analyses. GTR + I (0.6470) + G (0.5420) was the best-fit evolutionary model selected by jModeltest version 2.1.7 under the Akaike Information Criterion (Guindon and Gascuel, 2003;

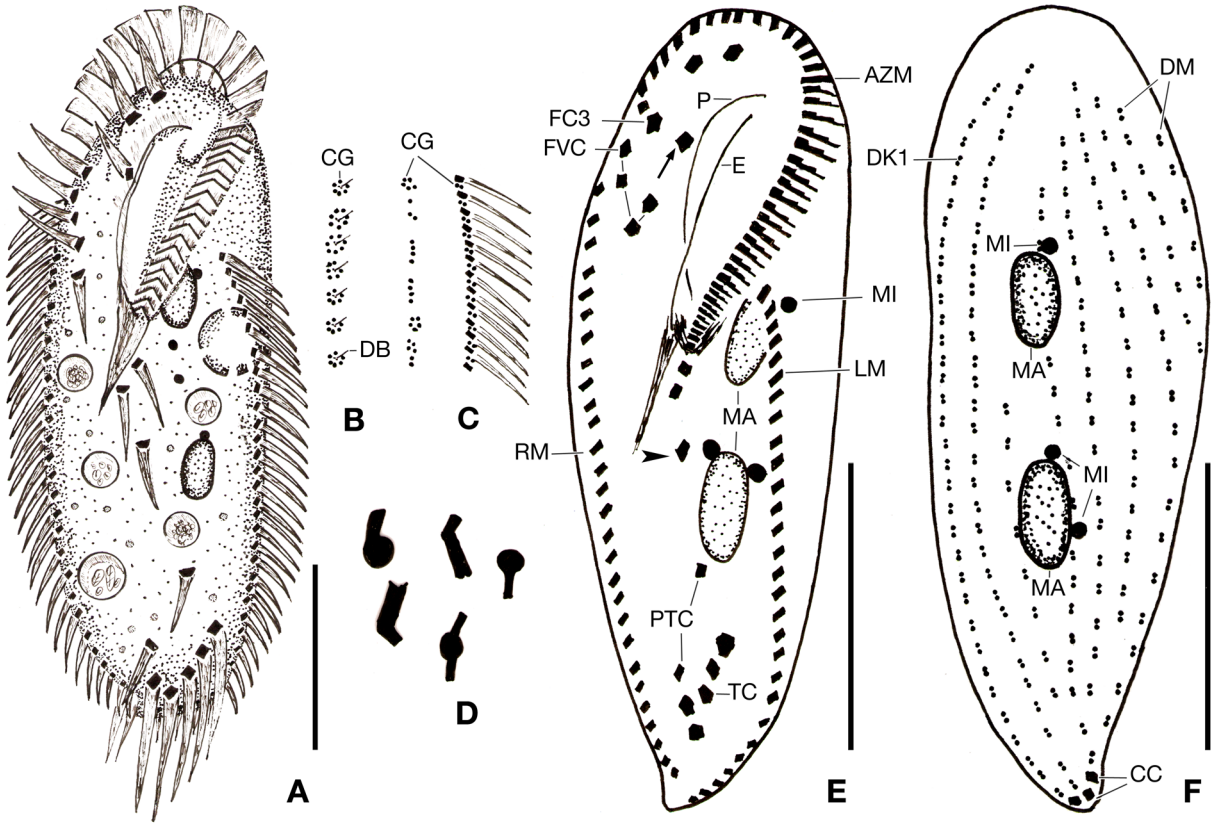

Fig. 1. The illustrations of *Australocirrus shii* (Shi et al.) from life (A–D) and after protargol impregnation (E, F). A, Ventral view of a representative specimen; B, C, Cortical granulation; D, Cytoplasmic crystals; E, F, Ventral and dorsal views of ciliature, arrow and arrowhead in E point to the buccal and posteriormost postoral cirrus, respectively. AZM, adoral zone of membranelles; CC, caudal cirri; CG, cortical granules; DB, dorsal bristle; DK1, dorsal kinety 1; DM, dorsomarginal rows; E, endoral membrane; FC3, frontal cirrus 3; FVC, frontoventral cirri; LM, left marginal row; MA, macronucleus; MI, micronucleus; P, paroral membrane; PTC, pretransverse ventral cirri; RM, right marginal row; TC, transverse cirri. Scale bars: A, E, F = 50 μm.

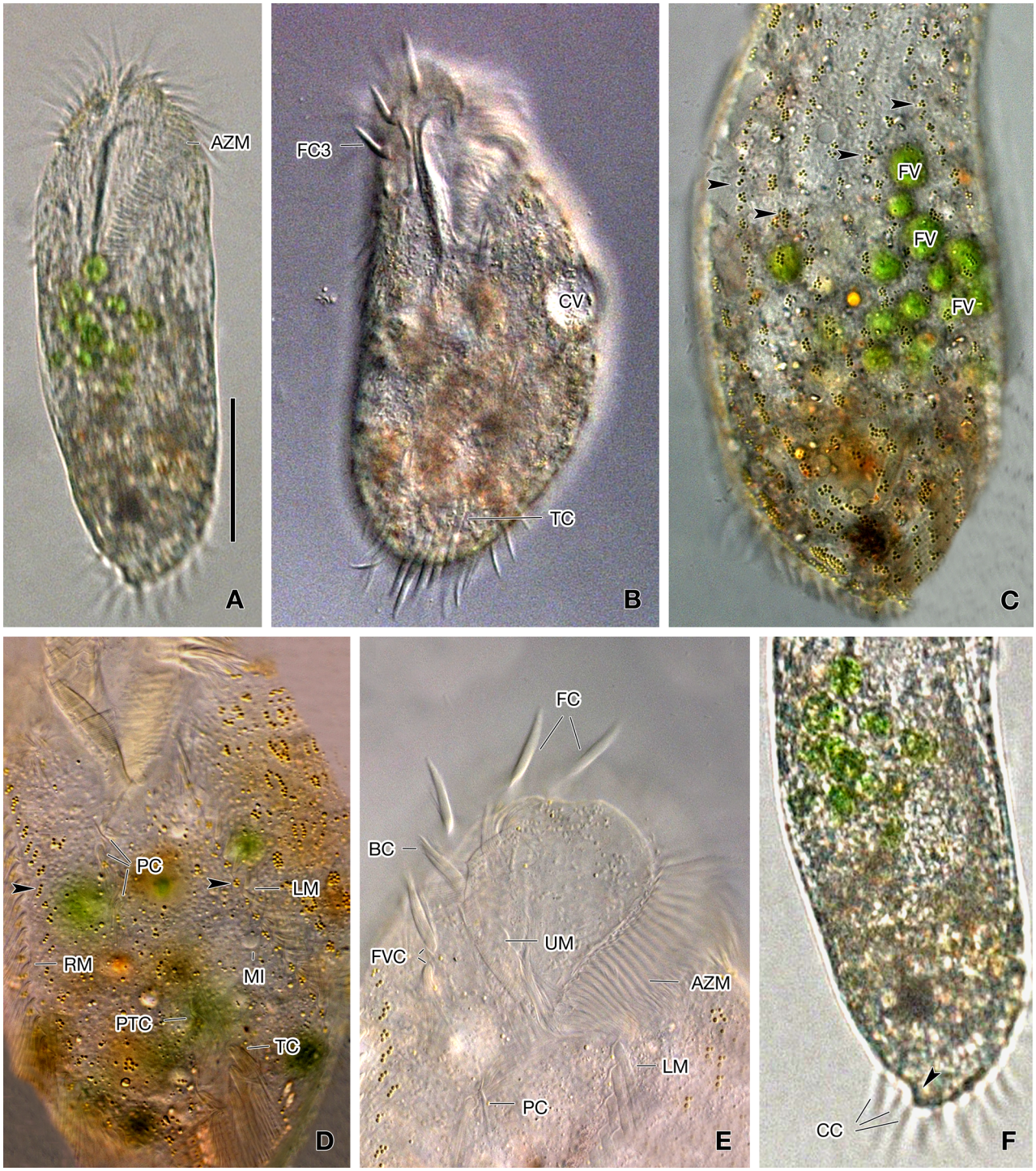

Fig. 2. Photomicrographs of *Australocirrus shii* (Shi et al.) from life. A, B, Ventral views of specimens, showing body shape and position of contractile vacuole; C, Arrowheads point to the rows of cortical granules on dorsal surface; D, E, Slightly squeezed specimens, showing ventral ciliature, cortical granules and micronuclei; F, Arrowhead marks the indent at the posterior body end. AZM, adoral zone of membranelles; BC, buccal cirrus; CC, caudal cirri; CV, contractile vacuole; FC, frontal cirri; FC3, frontal cirrus 3; FV, food vacuole; FVC, frontoventral cirri; LM, left marginal row; MI, micronucleus; PC, postoral cirri; PTC, pretransverse ventral cirri; RM, right marginal row; TC, transverse cirri; UM, undulating membranes. Scale bar: A = 50 μm.

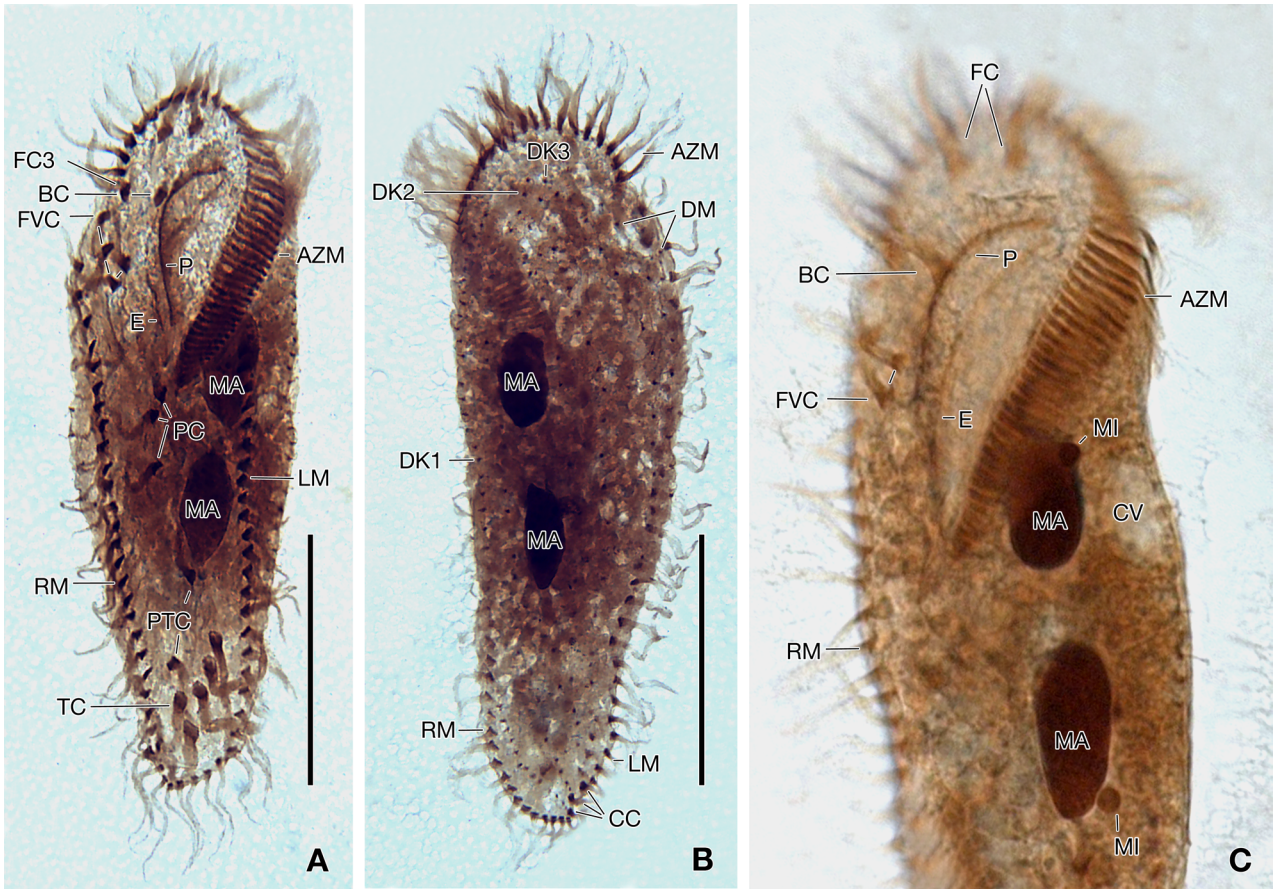

Fig. 3. Photomicrographs of *Australocirrus shii* (Shi et al.) after protargol impregnation. Ventral (A, C) and dorsal (B) view of voucher specimens, showing ciliature and nuclear apparatus. Note the position of anteriormost pretransverse ventral cirrus and arrangement of transverse cirri in two groups. AZM, adoral zone of membranelles; BC, buccal cirrus; CC, caudal cirri; CV, contractile vacuole; DK1–3, dorsal kineties 1–3; DM, dorsomarginal kineties; E, endoral membrane; FC, frontal cirri; FC3, frontal cirrus 3; FVC, frontoventral cirri; LM, left marginal row; MA, macronucleus; MI, micronucleus; P, paroral membrane; PC, postoral cirri; PTC, pretransverse ventral cirri; RM, right marginal row; TC, transverse cirri. Scale bars: A, B = 50 µm.

Posada, 2008). Bayesian inference (BI) analysis was carried out with MrBayes v3.1 (Ronquist and Huelsenbeck, 2003), using best-fit evolutionary model. Markov chain Monte Carlo (MCMC) simulations were run for 2,000,000 generations of which the first 5000 trees were burn-in and the remaining trees were used to calculate convergence by MrBayes until the average standard deviation of split frequencies reached below 0.01. Maximum likelihood (ML) analysis was performed using computer program PhyML version 3.0 (Guindon et al., 2010) (http://www.atgc-montpellier.fr/phyml/). Nonparametric bootstrap method with 1,000 replicates was used to evaluate the reliability of internal branches. Phylogenetic trees were visualized using the free software package FigTree v1.4 by A. Rambaut at http://tree.bio.ed.ac.uk/software/figtree/. Subclass Oligotrichia was selected as out group taxa in the phylogenetic tree analyses.

SYSTEMATIC ACCOUNTS

Order Sporadotrichida Fauré-Fremiet, 1961
Family Oxytrichidae Ehrenberg, 1830
Genus *Australocirrus* Blatterer & Foissner, 1988

***Australocirrus shii* (Shi et al., 1997) Kumar & Foissner, 2015 (Tables 1, 3, Figs. 1–3)**

Description of the Korean population. Body size *in vivo* 100–200 × 40–80 µm, on average 175 × 65 µm; usually about 115–170 × 35–60 µm after protargol impregnation. Body shape elongate to ellipsoidal or slightly elongate obovate; dorsoventrally flattened about 2 : 1. Macronucleus slightly left of mid-body, composed of two macronuclear nodules, on average 16 × 8 µm in size (Fig. 3A, B), about three micronuclei attached to the macronuclear nodules,

Table 2. Morphometric data of *Afrokeronopsis aurea* Korean population

Characters	Mean	M	SD	SE	CV	Min	Max	n
Body, length	208.2	207.5	40.7	9.1	0.2	135.0	272.0	20
Body, width	73.3	69.5	14.4	3.2	0.2	54.0	106.0	20
Body length : width, ratio	2.8	2.8	0.3	0.1	0.1	2.3	3.3	20
AZM, length	85.5	88.5	13.1	2.9	0.2	63.0	107.0	20
AZM length : body length, ratio	2.4	2.3	3.1	3.1	1.3	2.1	2.5	20
Buccal field, maximum width	19.1	19.5	5.7	1.3	0.3	8.0	30.0	20
Anterior body end to RM, distance	78.5	81.0	16.7	3.7	0.2	38.0	103.0	20
Anterior body end to LM, distance	62.6	60.5	13.8	3.1	0.2	43.0	86.0	20
Anterior body end to FTC, distance	67.6	69.0	15.6	3.5	0.2	39.0	95.0	20
Anterior body end first midventral cirri, distance	73.4	72.5	11.0	2.5	0.1	57.0	91.0	20
Anterior body end anteriormost TC, distance	94.1	93.0	18.6	4.1	0.2	61.0	138.0	20
Midventral rows in mid-body, distance in between	6.9	7.0	1.3	0.3	0.2	5.0	10.0	20
Posterior body end to posteriormost TC, distance	10.2	10.5	3.5	0.8	0.3	2.0	16.0	20
Anterior body end to first MA, distance	57.5	57.5	13.4	3.0	0.2	31.0	80.0	20
MA nodules, distance in between	25.6	24.0	10.2	2.3	0.4	10.0	42.0	20
Anterior MA nodule, length	28.0	27.0	6.3	1.4	0.2	20.0	41.0	20
Anterior MA nodule, width	13.8	14.0	2.3	0.5	0.2	8.0	18.0	20
Posterior MA nodule, length	31.4	30.0	8.3	1.8	0.3	20.0	47.0	20
Posterior MA nodule, width	13.0	13.0	2.4	0.5	0.2	10.0	20.0	20
AM, number	94.9	96.5	11.5	2.6	0.1	72.0	110.0	20
MA nodules, number	2.3	2.0	0.6	0.1	0.2	2.0	4.0	20
FC, number	12.2	12.0	2.1	0.5	0.2	9.0	17.0	20
BC, number	6.4	6.0	1.5	0.3	0.2	4.0	10.0	20
FTC, number	2.0	2.0	0.0	0.0	0.0	2.0	2.0	20
MP, number	30.8	32.0	4.1	1.0	0.1	24.0	38.0	20
TC, number	20.1	20.0	1.6	0.4	0.1	18.0	24.0	20
RMC, number	37.7	38.0	4.0	1.0	0.1	29.0	44.0	20
LMC, number	43.7	44.5	4.4	1.0	0.1	34.0	53.0	20
CC, number	3.0	3.0	0.0	0.0	0.0	3.0	3.0	20
DK, number	14.4	15.0	3.1	0.7	0.2	9.0	17.0	20
PTC, number	1.0	1.0	0.0	0.0	0.0	1.0	1.0	20
Posterior body end and LM, distance	7.1	6.5	1.7	0.4	0.2	5.0	10.0	20
Distance between BC	4.4	4.0	0.7	0.2	0.2	3.0	6.0	20
Distance between FC	5.2	5.0	1.0	0.2	0.2	4.0	8.0	20
Posterior MA and posterior body end, distance	67.2	64.5	20.1	4.5	0.3	39.0	124.0	20
MI, number	0.1	0.0	0.2	0.1	4.5	0.0	1.0	20
FVC, number	4.4	4.0	0.5	0.1	0.1	4.0	5.0	20

Data based on mounted, protargol-impregnated, and randomly selected specimens from a nonflooded Petri dish culture. Measurements of length or width or distance in μm.

Mean, arithmetic mean; M, median; SD, standard deviation; SE, standard error of arithmetic mean; CV, coefficient of variation in %; Min, minimum; Max, maximum; n, number of individuals investigated; AM, adoral membranelles; AZM, adoral zone of membranelles; BC, buccal cirrus; CC, caudal cirri; DK, dorsal kineties; FC, frontal cirrus; FTC, frontoterminal cirri; FVC, frontoventral cirri; LM, left marginal row; LMC, left marginal cirri; MA, macronucleus; MI, micronucleus; MP, mid ventral cirral pairs; PTC, pre transverse cirri; RM, right marginal row; RMC, right marginal cirri; TC, transverse cirri.

each about 3 μm in diameter (Figs. 1F, 3C). Contractile vacuole located slightly above mid-body near left cell margin, about 20 μm across during diastole, with lacunar collecting canals (Figs. 2B, 3C). Cortical granules citrine yellowish, arranged longitudinally along cirral rows and dorsal kineties, about 1 μm across (Fig. 2C, D). Cell colorless but dark at lower magnification because of opaque cytoplasm (Fig. 2A). Light microscopic observation reveals brown spots on body due to foods (Fig. 2A–C). Lipid droplets usually brownish, scattered throughout cytoplasm; few small crystals mainly in posterior body (Figs. 1D, 2C). Food vacuoles greenish because of algae, 10–25 μm across (Fig. 2C, D). Swims and glides rather rapidly.

Three frontal cirri slightly enlarged, about 20 μm long (Figs. 1E, 2B, E, 3A, C). Four frontoventral cirri, about 17 μm long (Figs. 1E, 2E, 3A). Postoral ventral cirri three, posterior most cirrus near mid-body, about 17 μm long (Figs. 1E, 2D, 3A). Two pretransverse cirri obliquely arranged; distance between anterior pretransverse cirrus and anterior most transverse cirrus about 12 μm (Figs. 1E, 2D, 3A). Five slightly hypertrophied transverse cirri arranged in two groups (3 + 2), about 35 μm long (Figs. 1E, 3A). Three cau-

Table 3. Comparisons between local populations of *Australocirrus shii* and *Afrokeronopsis aurea*

Characters	*Australocirrus shii*					*Afrokeronopsis aurea*	
	Korea	Australia	China	India	Korea	Korea	South Africa
Body length	139.6	169.0	175.0	138.3	252.3	208.2	306.4
Body width	43.8	50.0	63.0	51.2	102.0	73.3	111.8
Body length : width ratio	3.2	3.4	–	2.7	2.5	2.8	2.8
AM number	47.9	50.0	2.8	50.4	57.1	94.9	100.3
MA nodules number	2.0	2.0	33.0	2.0	2.0	2.0	2.0
MI number	2.9	31.0	31.0	4.9	5.9	2.0	-
Indent at posterior body end	yes	no	no	yes	no	no	no
LMC number	28.5	36.0	33.0	29.6	35.2	43.7	58.2
RMC number	28.2	31.0	31.0	29.1	27.5	37.6	50.4
FC number	3.0	3.0	3.0	3.1	3.0	12.2	12.8
TC number	5.0	5.0	5.0	5.0	5.0	20.1	23.9
Arrangement of TC	**3+2**	**3+2**	**3+2**	**3+2**	**3+2**		
FVC number	4.1	4.0	4.0	4.2	4.0	4.4	4.0
DK number	8.6	10.0	8.0	8.7	7.5	14.4	14.1
CC number	**3.0**	**3.0**	**3.0**	**3.0**	**3.0**	**3.0**	**3.0**
MP number	3.0	3.0	3.0	3.2	3.0	30.8	37.9
Data sources	Present study	Kumar and Foissner (2015)	Shi et al. (1997)	Singh et al. (2013)	Kim et al. (2012)	Present study	Foissner and Stoeck (2008)

All measurements of length or width are in micrometer (μm). Important features are in bold. Average data of protargol impregnated and randomly selected specimens.
AM, adoral membranelles; CC, caudal cirri; DK, dorsal kineties; FC, frontal cirrus; FVC, frontoventral cirri; LMC, left marginal cirri; MA, macronucleus; MI, micronucleus; MP, mid ventral cirral pairs; RMC, right marginal cirri; TC, transverse cirri.

dal cirri (Figs. 1F, 3B). Marginal cirri in two non-confluent posterior rows about 20 μm long, size of marginal cirri gradually decreasing towards posterior end; left row extending around posterior margin (Figs. 1E, 2D, 3A). Eight ornine dorsal kineties; dorsal bristles 4–5 μm long.

Conspicuous buccal area, large and deep (Fig. 2A, B). Adoral zone of membranelles about 30% of cell length with 40–55 membranelles, cilia up to 17 μm long (Fig. 2A, E). One buccal cirrus about 16 μm long (Figs. 1E, 2E, 3A). Undulating membranes in *Australocirrus* pattern intersect near rear end of paroral membrane (Figs. 1E, 3A, C). Pharyngeal fibres extends obliquely backwards after impregnation about 30 μm long (Fig. 1E).

Distribution. Australia, China, India, Korea (present study).

Remarks. Most of the morphometric characteristics of the Korean population of *Au. shii* overlap with those of Australian, Chinese, and Indian populations. The Korean population was previously described as *Cyrtohymena australis* by Kim et al. (2012) and the Indian population was described as *C.* (*Cyrtohymenides*) *shii* by Singh et al. (2013); however, Kumar and Foissner (2015) synonymized both Indian and Korean populations with *Au. shii* based on the following characteristics, i.e., distance between the anterior pretransverse cirrus and the anteriormost transverse cirrus; arrangement of transverse cirri; and resting cyst. The present Korean population of *Au. shii* is similar in ciliature with the original description but differs from body size and presence of an indentation at posterior end (Shi et al., 1997; Kumar and Foissner, 2015). However, these morphological variations could be the result of different environmental conditions.

The dorsal ciliature of *C. australis* sensu Kim et al. (2012) is more similar to *C. muscorum* (Kahl, 1932) Foissner, 1989 and significantly different from the present Korean population of *Au. shii* thus we beleive that Kim et al. (2012) misinterpret the dorsal ciliature of *C. australis* therefore a corrected dorsal ciliature pattern has been provided in this study.

Family Neokeronopsidae Foissner & Stoeck, 2008
Genus *Afrokeronopsis* Foissner et al., 2010

***Afrokeronopsis aurea* (Foissner & Stoeck, 2008) Foissner et al., 2010 (Tables 2, 3, Figs. 4–6)**

Description of the Korean population. Body size *in vivo* 230–375 × 70–145 μm, on average 300 × 100 μm; specimens shrunk considerably after staining, i.e., 135–275 × 55–105 μm. Body shape elongate obovate or ellipsoidal, broadest in mid-body, posterior end narrowly rounded to bluntly pointed (Fig. 5A). Body dorsoventrally flattened. Macronuclear nodules widely apart, anterior onelocated at level of proximal end of adoral zone of membranelles, elongate to ellipsoidal shape, size: 20–41 × 8–18 μm, other one located near midbody, size: 20–47 × 10–20 μm (Figs. 5B, 6A, G) and two macronuclear nodules connected by a fine strand

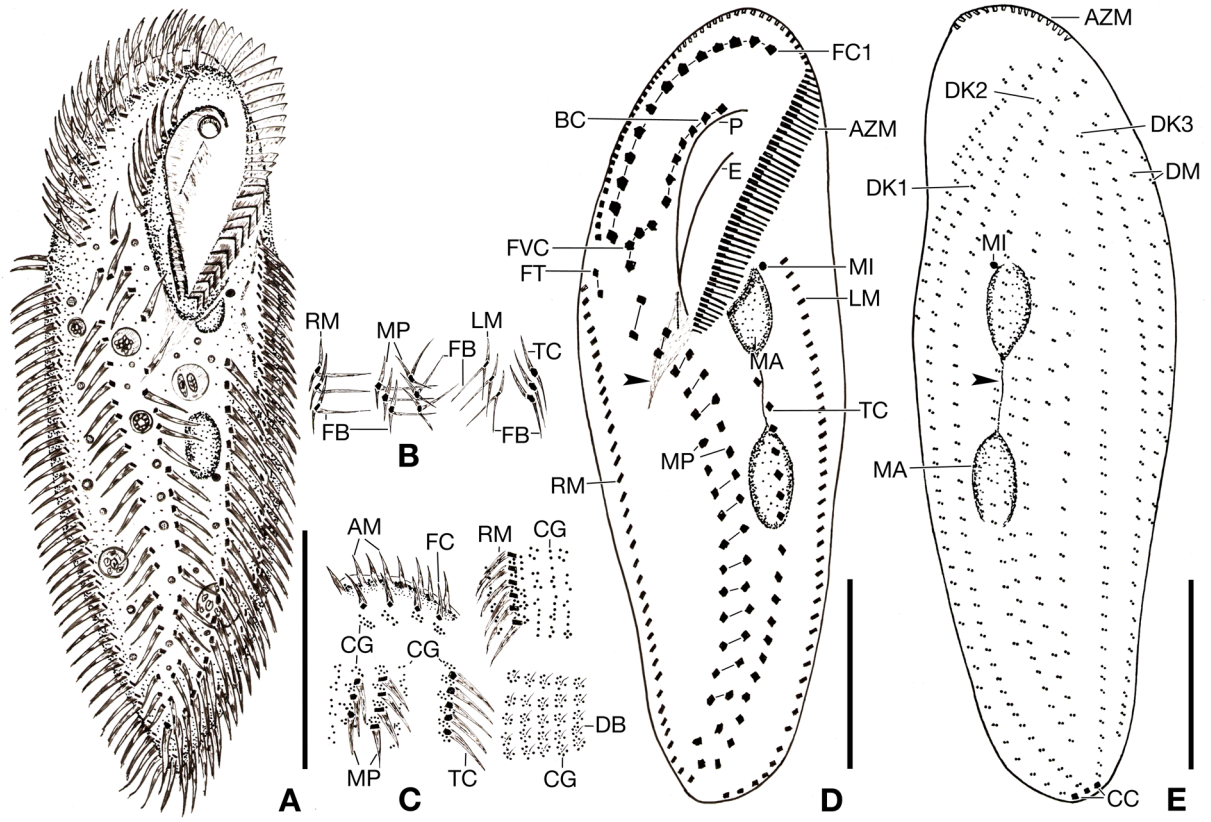

Fig. 4. The illustrations of *Afrokeronopsis aurea* (Foissner & Stoeck) from life (A–C), after protargol impregnation (D, E). A, A representative specimen; B, Associated fibers are present around the marginal cirri, midventral cirral pairs and transverse cirri; C, Small clusters of cortical granules are present at the base of the frontal cirri, marginal cirri, midventral cirral pairs, transverse cirri and dorsal bristles; D, E, Ventral and dorsal views of the voucher specimens, showing the ciliature and the nuclear apparatus, arrowhead in (D) points to the pharyngeal fiber, in (E) to the connecting macronuclear strand. AM, adoral membranelles; AZM, adoral zone of membranelles; BC, buccal cirrus; CC, caudal cirri; CG, cortical granules; DB, dorsal bristle; DK1–3, dorsal kineties 1–3; DM, dorsomarginal rows; E, endoral membrane; FB, fibers; FC, frontal cirri; FC1, frontal cirrus 1; FVC, frontoventral cirri; FT, frontoterminal cirri; LM, left marginal row; MA, macronucleus; MI, micronucleus; MP, midventral cirral pairs; P, paroral membrane; RM, right marginal row; TC, transverse cirri. Scale bars: A = 100 μm, D, E = 50 μm.

recognizable only in protargol stained specimens (Fig. 6A); One or two micronuclei attached to macronuclear nodules, rarely noticeable (Fig. 6G). Contractile vacuole, conspicuously above mid-body near left cell margin, with lacunar collecting canals (Fig. 5A arrowhead). Citrine yellow cortical granules arranged longitudinally, along cirral rows and dorsal kineties, ellipsoid to obovate, 1.5–2 μm across (Fig. 5D, G). Four to ten granules formed brick-shaped aggregate at the base of each frontal cirri (Figs. 4C, 5C). Color of cells dark at lower magnification corresponding with higher magnification but colorless or sometime golden yellow to brown orange under light microscope (Fig. 5A, B, E). Lipid droplets spreaded on cytoplasm, 2–4 μm in diameter (Fig. 5H). Food vacuoles up to 40 μm across, containing algae, diatoms, flagellates, and bacteria (Fig. 5B, H). Swims and glides rapidly sometime crawling on debris.

Cirri associated with complex fiber system very similar in all rows, but slightly different in case of transverse cirri (Fig. 4B, C). Most of cirri usually 18–25 μm long, except of enlarged frontal cirri, buccal cirri and transverse cirri. Frontal cirri and adoral membranelles formed an apical corona (Figs. 4A, D, 6B, H). Two frontoterminal cirri below distal end of adoral zone of membranelles and close to midventral cirral pairs (Fig. 4D). Midventral complex composed of cirral pairs about 7 μm apart in mid-body (Figs. 4D, 6E, F). On an average 20 transverse cirri about 30 μm long, commencing beneath level of buccal vertex and extending around last midventral cirri forming a J-shaped row slightly left side of mid-body axis (Figs. 4D, 5F, 6E, F). Both marginal rows commenced slightly above level of buccal vertex; left marginal row J-shaped curving around body posterior end almost touching right marginal row (Fig. 4D). About 9–17

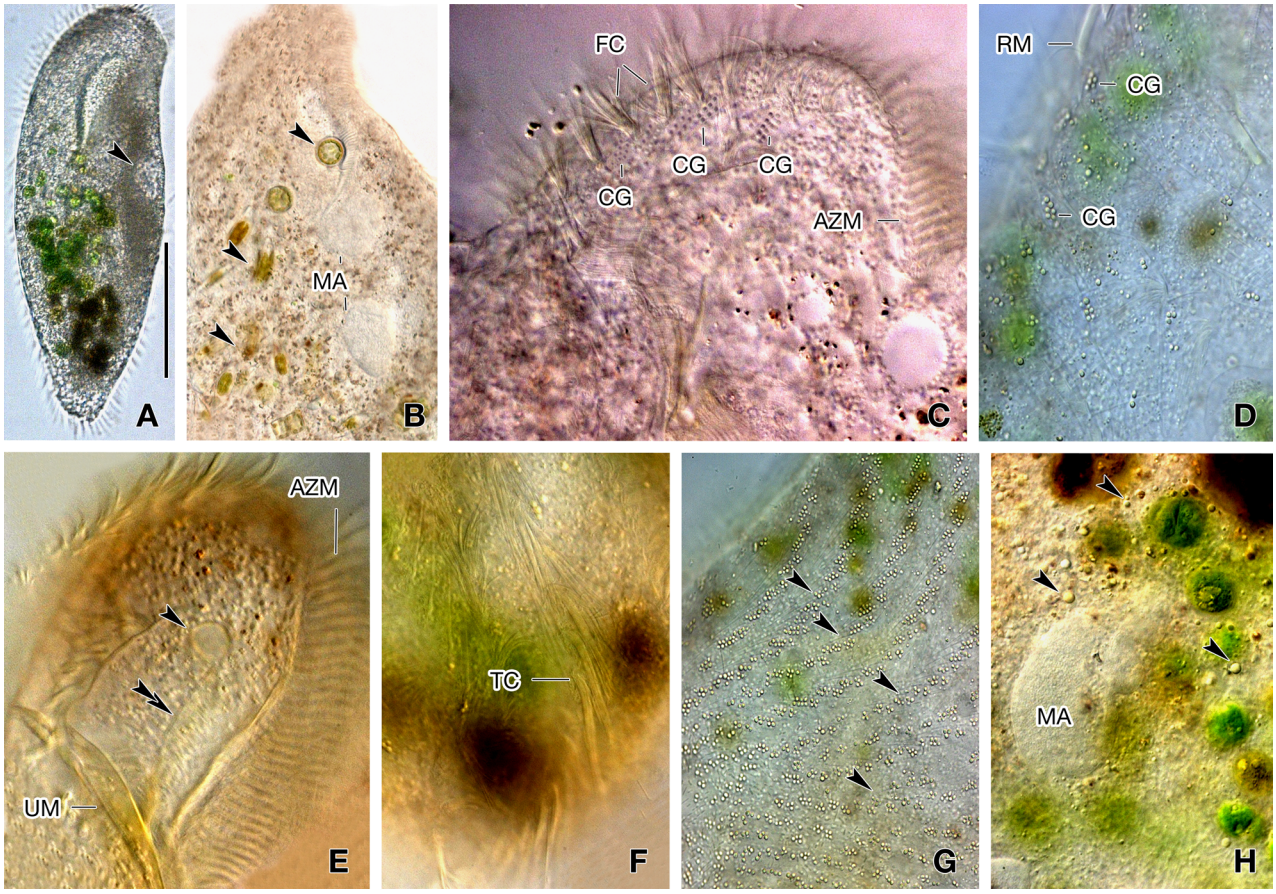

Fig. 5. Photomicrographs of *Afrokeronopsis aurea* (Foissner & Stoeck) from life. A, Ventral view of a specimen, showing body shape and position of contractile vacuole (arrowhead); B, H, Sections, showing food vacuoles (arrowheads in B) and nuclear apparatus, arrowheads in H point to the lipid droplets; C, cortical granules are arranges in small clusters at the base of the frontal cirri; D, G, cortical granulations, arrowheads in G marks the granules arranged in rows; E, Arrowhead marks the buccal depression, double arrowhead to the endoral membrane; F, Section, showing the transverse cirri. AZM, adoral zone of membranelles; CG, cortical granules; FC, frontal cirri; MA, macronucleus; RM, right marginal row; TC, transverse cirri; UM, undulating membranes. Scale bar: A = 100 µm.

dorsal kineties including several short kineties, most of them extending from anterior to posterior body end; dorsal bristle 2–4 µm long (Figs. 4E, 6D). At posterior body end, gap between marginal rows dorsally occupied by caudal cirri (Figs. 4E, 6C). Adoral zone of membranelles U-shaped occupying almost 35%–40% of body length with 72–110 membranelles, length of cilia up to 16–23 µm (Figs. 5E, 6B).

Buccal area conspicuous, long and deep (Figs. 5A, 6B). Undulating membranes *Australocirrus* type (Fig. 6B, H) and buccal depression as a strongly curved elongation of the paroral membrane (Figs. 4A, 6H). A fiber observed just below the buccal depression (Figs. 4A, 5E). Buccal cirri closely located along undulating membranes, and 4–10 in number (Figs. 4D, 6B, H).

Distribution. South Africa, South Korea (present study).

Remarks. Most of the morphometric characteristics of the Korean population of *Af. aurea* are overlapped with those of South African population, except for the lower numbers of marginal and midventral cirri in Korean population (Table 3). However, the body length and width ratio is similar in protargol stained specimens (Table 3), which implies these variations are insignificant (Foissner and Stoeck, 2008). So far, two species are described under the genus *Neokeronopsis*, namely, *N. asiatica* Foissner, Shi, Wang and Warren, 2010 and *N. spectabilis* (Kahl, 1932), importantly both species lack buccal depression that is considered as a generic character of the genus *Afrokeronopsis*. The Korean population of *Af. aurea* has a buccal depression thus its identification under the genus *Afrokeronopsis* is in no doubt. Furthermore, *Af. aurea* could be distinguished from *N. spectabilis* and *N. asiatica* by the number of caudal cirri (Warren et al., 2002; Wang et al., 2007; Foissner and Stoeck, 2008; Jung et al., 2015) (Table 3).

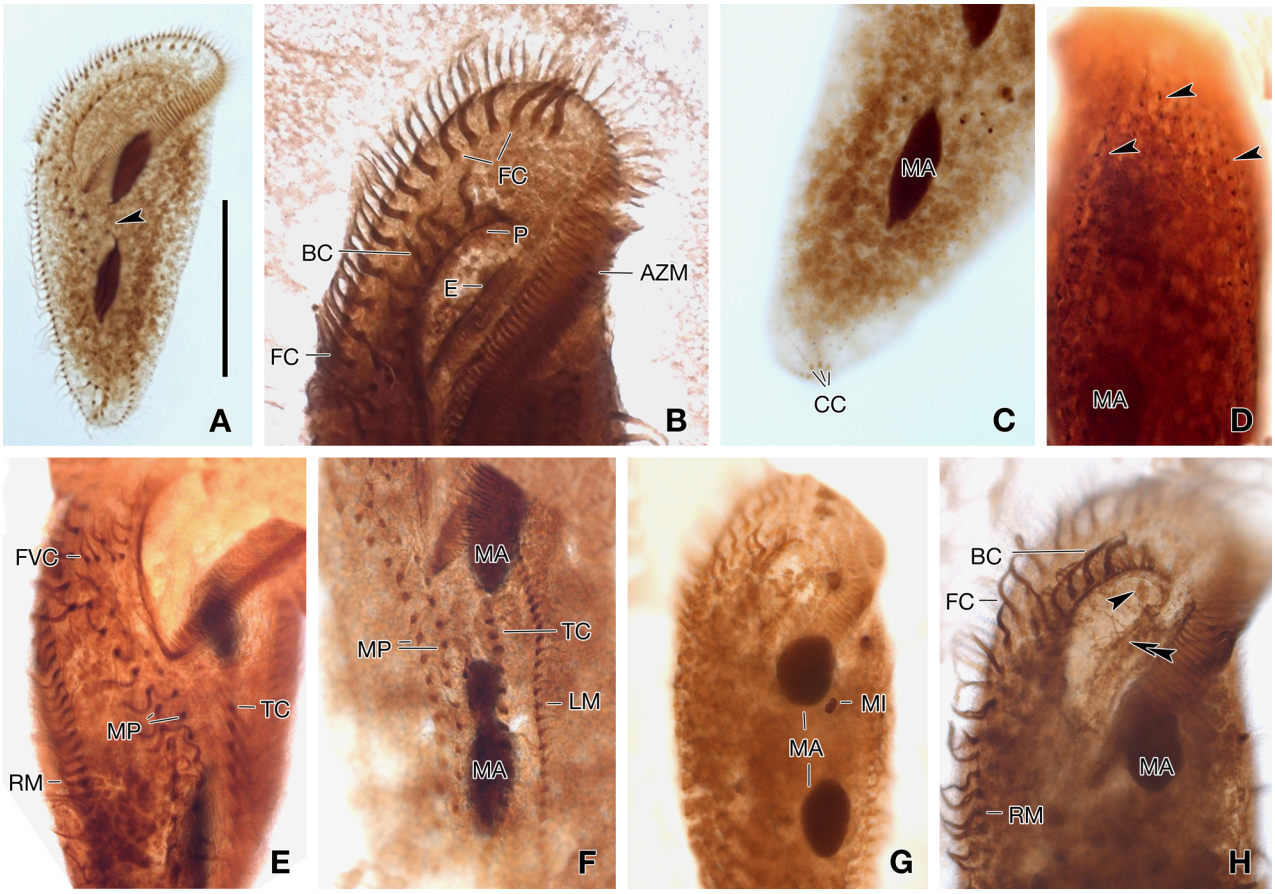

Fig. 6. Photomicrographs of *Afrokeronopsis aurea* (Foissner & Stoeck) after protargol impregnation. A, Ventral view of a specimen, showing the ciliature, arrowhead points to the macronuclear strand; B, E–H, Ciliature and nuclear apparatus on the ventral surface, arrowhead in H points to the buccal depression visible in stained preparation, double arrowhead points to the light stained endoral membrane; C, D, Ciliature on the dorsal surface, arrowheads in D point to the dorsal kinety rows. AZM, adoral zone of membranelles; BC, buccal cirrus; CC, caudal cirri; E, endoral membrane; FC, frontal cirrus; FVC, frontoventral cirri; LM, left marginal row; MA, macronucleus; MI, micronucleus; MP, midventral cirral pairs; P, paroral membrane; RM, right marginal row; TC, transverse cirri. Scale bar: A = 100 µm.

18S rRNA gene sequences and phylogenetic analyses (Fig. 7). Length of sequence, GC content and GenBank accession number of newly sequenced 18S rRNA gene of *Australocirrus shii* and *Afrokeronopsis aurea* are 1,678 bp, 45.2%, KY968740 and 1,690 bp, 44.6%, KY968741, respectively. Phylogenetic analyses such as ML and BI generated almost similar tree topologies, thus ML tree has been shown with posterior probability values from BI and bootstrap values from ML analyses. All populations of *Au. shii* clustered with American populations of *Cyrtohymena citrina* but not with Namibian and Indian populations of *C. citrina*. *Neokeronopsis asiatica* grouped with *Au. shii* and American populations of *C. citrina* as sister clade. *Apoterritricha lutea* Kim, Vdačný, Shazib and Shin, 2014 interconnected *N. asiatica* and it's sister clade. Two populations of *Af. aurea* were grouped together with all Neokeronopsidae members (*Ap. lutea*, *N. asiatica*, and *Af. aurea*), and form a non-monophyletic family clade.

Remarks on phylogeny. In our phylogenetic analyses, newly sequenced Korean population of *Au. shii* grouped with the Indian population of *Au. shii* and two American populations of *C. citrina* with moderate support (ML 72%, BI 0.96) (Fig. 7). Interestingly, *N. asiatica* grouped with *Au. shii* and *C. citrina* clade with moderate support from both trees (ML 74%, BI 0.90) (Fig. 7). The non-monophyly of Neokeronopsids with *Au. shii* has been reported in several literatures (Singh et al., 2013; Kim et al., 2014; Shao et al., 2014; Jung et al., 2015; Kumar et al., 2017) which is in agreement with the present study. Despite a substantial morphological difference among *N. asiatica*, *Au. shii* and *C. citrina*, *N. asiatica* clustered with them in the phylogenetic tree. Moreover, the 18S rRNA gene sequence of *N. asiatica* differs from

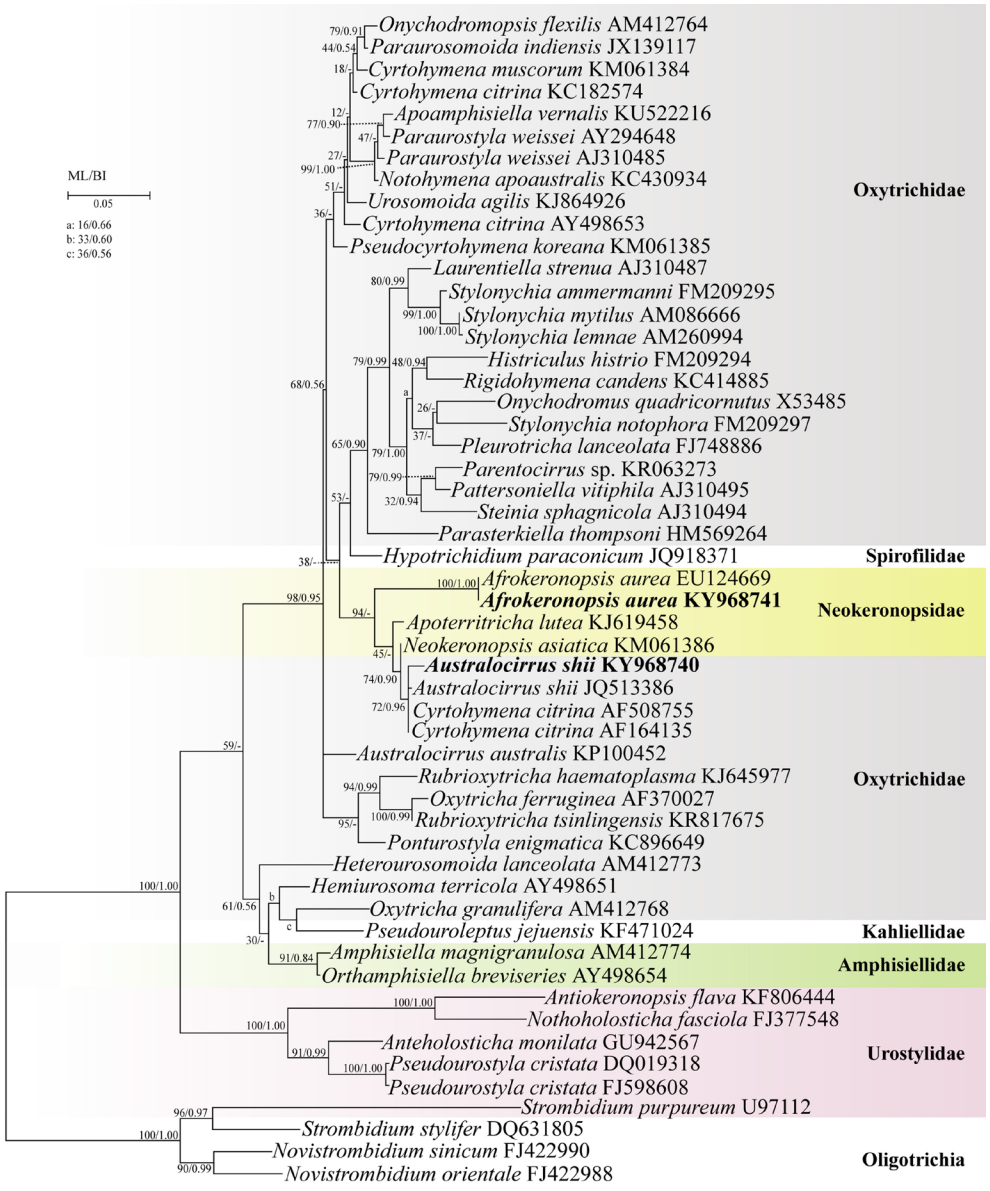

Fig. 7. 18S rRNA gene phylogeny inferred from the ClustalW alignment employing 53 taxa and 1,671 nucleotide characters. Results from Bayesian inference (BI) analysis are mapped onto the maximum likelihood (ML) tree. Codes following names are GenBank accession numbers. Numbers at nodes represent bootstrap values of ML out of 1,000 replicates and posterior probability of Bayesian analysis (BI). A hypen (-) represents minor differences between Bayesian and ML tree topologies. Scale bar corresponds to five substitutions per 100 nucleotide positions.

those of Korean and Indian populations of *Au. shii* by only two and three nucleotides, respectively (Table 4). Recently, Kumar and Foissner (2015) provided a helpful review on the undulating membranes (UM) patterns of typical 18 cirri oxytrichid genera. Our observations along with data from Kumar and Foissner (2015) show that UM pattern of *N. asiatica* is *Australocirrus* type which indicate that species possessing *Australocirrus* UM pattern make a clade sparsely. Furthermore, we agree that the shape of the UM especially

Table 4. Pairwise distance (in %, above diagonal) and numbers of nucleotide differences (below diagonal) of the 18S rRNA gene sequences among five species

Species	1	2	3	4	5
1 *Australocirrus shii* JQ513386	–	99.9	99.8	98.2	98.2
2 ***Australocirrus shii***	1	–	99.9	98.2	98.2
3 *Neokeronopsis asiatica* KM061386	3	2	–	98.1	98.1
4 ***Afrokeronopsis aurea***	29	28	30	–	100
5 *Afrokeronopsis aurea* EU124669	29	28	30	0	–

Newly sequenced species are in bold.

paroral membrane have some phylogenetic significance and it has evolved convergently several times (Jung et al., 2015; Kumar and Foissner, 2015). Jung et al. (2015) mentioned that phylogenetic relationships are still problematic in the groups possessing UM of *Cyrtohymena* pattern. In addition to that 18S rRNA gene sequences are supposed to be insufficient for separating different species of the genera *Neokeronopsis* and *Australocirrus* (Kim et al., 2013; Huang et al., 2014; Tsai et al., 2015). Moreover, multigene analyses are more preferable to resolve such problems (Huang et al., 2012, 2014).

ACKNOWLEDGMENTS

The present study was supported by the National Institute of Biological Resources (NIBR) funded by the Ministry of Environment (NIBR201702101), and the National Research Foundation of Korea funded by the Korean government of Ministry of Education, and Ministry of Science and ICT (2015R1D1A09058911, 2015H1D3A1062066). We appreciate anonymous reviewers who gave comments and suggestions to improve the manuscript.

REFERENCES

Ammermann D, Steinbrück G, von Berger L, Hennig W, 1974. The development of the macronucleus in the ciliated protozoan *Stylonychia mytilus*. Chromosoma, 45:401-429.

Berger H, 1999. Monograph of the Oxytrichidae (Ciliophora, Hypotrichia). Monographiae Biologicae. Vol. 78. Kluwer Academic Publishers, Dordrecht, pp. 1-1080.

Blatterer H, Foissner W, 1988. Beitrag zur terricolen Ciliatenfauna (Protozoa: Ciliophora) Australiens. Stapfia, 17:1-84.

Castresana J, 2000. Selection of conserved blocks from multiple alignments for their use in phylogenetic analysis. Molecular Biology and Evolution, 17:540-552. https://doi.org/10.1093/oxfordjournals.molbev.a026334

Foissner W, 2004. Some new ciliates (Protozoa, Ciliophora) from an Austrian floodplain soil, including a giant, red "flagship", *Cyrtohymena* (*Cyrtohymenides*) *aspoecki* nov. subgen., nov. spec. Denisia, 13:369-382.

Foissner W, Moon-van der Staay SY, van der Staay GWM, Hackstein JHP, Krautgartner WD, Berger H, 2004. Reconciling classical and molecular phylogenies in the stichotrichines (Ciliophora, Spirotrichea), including new sequences from some rare species. European Journal of Protistology, 40:265-281. https://doi.org/10.1016/j.ejop.2004.05.004

Foissner W, Shi X, Wang R, Warren A, 2010. A reinvestigation of *Neokeronopsis* populations, including the description of *N. asiatica* nov. spec. (Ciliophora, Hypotricha). Acta Protozoologica, 49:87-105.

Foissner W, Stoeck T, 2008. Morphology, ontogenesis and molecular phylogeny of *Neokeronopsis* (*Afrokeronopsis*) *aurea* nov. subgen., nov. spec. (Ciliophora: Hypotricha), a new African flagship ciliate confirms the CEUU Hypothesis. Acta Protozoologica, 47:1-33.

Guindon S, Dufayard JF, Lefort V, Anisimova M, Hordijk W, Gascuel O, 2010. New algorithms and methods to estimate maximum-likelihood phylogenies: assessing the performance of PhyML 3.0. Systematic Biology, 59:307-321. https://doi.org/10.1093/sysbio/syq010

Guindon S, Gascuel O, 2003. A simple, fast, and accurate algorithm to estimate large phylogenies by maximum likelihood. Systematic Biology, 52:696-704. https://doi.org/10.1080/10635150390235520

Huang J, Chen Z, Song W, Berger H, 2014. Three-gene based phylogeny of the Urostyloidea (Protista, Ciliophora, Hypotricha), with notes on classification of some core taxa. Molecular Phylogenetics and Evolution, 70:337-347. https://doi.org/10.1016/j.ympev.2013.10.005

Huang J, Dunthorn M, Song W, 2012. Expanding character sampling for the molecular phylogeny of euplotid ciliates (Protozoa, Ciliophora) using three markers, with a focus on the family Uronychiidae. Molecular Phylogenetics and Evolution, 63:598-605. https://doi.org/10.1016/j.ympev.2012.02.007

Jung JH, Park KM, Min GS, 2015. Morphology and molecular phylogeny of *Pseudocyrtohymena koreana* n.g., n. sp. and antarctic *Neokeronopsis asiatica* Foissner et al., 2010 (Ciliophora, Sporadotrichida), with a brief discussion of the *Cyrtohymena* undulating membranes pattern. Journal of Eukaryotic Microbiology, 62:280-297. https://doi.org/10.1111/jeu.12179

Kamra K, Sapra GR, 1990. Partial retention of parental ciliature during morphogenesis of the ciliate *Coniculostomum monilata* (Dragesco and Njiné, 1971) Njiné, 1978 (Oxytrichidae, Hypotrichida). European Journal of Protistology, 25:264-278. https://doi.org/10.1016/S0932-4739(11)80179-3

Kearse M, Moir R, Wilson A, Stones-Havas S, Cheung M, Sturrock S, Buxton S, Cooper A, Markowitz S, Duran C, Thierer T, Ashton B, Meintjes P, Drummond A, 2012. Geneious basic: an integrated and extendable desktop software platform for the organization and analysis of sequence data. Bioinformatics, 28:1647-1649. https://doi.org/10.1093/bioinformatics/bts199

Kim JH, V'dačný P, Shazib SUA, Shin MK, 2014. Morphology and molecular phylogeny of *Apoterritricha lutea* n. g., n. sp. (Ciliophora, Spirotrichea, Hypotrichia): a putative missing link connecting *Cyrtohymena* and *Afrokeronopsis*. Journal of Eukaryotic Microbiology, 61:520-536. https://doi.org/10.1111/jeu.12131

Kim SY, Choi JK, Dolan JR, Shin HC, Lee S, Yang EJ, 2013. Morphological and ribosomal DNA-based characterization of six antarctic ciliate morphospecies from the Amundsen Sea with phylogenetic analyses. Journal of Eukaryotic Microbiology, 60:497-513. https://doi.org/10.1111/jeu.12057

Kim YU, Lee JM, Kwon CB, Shin MK, 2012. Morphological redescriptions of three *Cyrtohymena* ciliates (Ciliophora: Sporadotrichida: Oxytrichidae) new to Korea. Journal of Species Research, 1:78-86.

Kumar S, Bharti D, Shazib SUA, Shin MK, 2017. Discovery of a new hypotrich ciliate from petroleum contaminated soil. PloS One, 12:e0178657. https://doi.org/10.1371/journal.pone.0178657

Kumar S, Foissner W, 2015. Biogeographic specializations of two large hypotrich ciliates: *Australocirrus shii* and *A. australis* and proposed synonymy of *Australocirrus* and *Cyrtohymenides*. European Journal of Protistology, 51:210-228. https://doi.org/10.1016/j.ejop.2015.02.002

Li L, Huang J, Song W, Shin MK, Al-Rasheid KAS, Berger H, 2010. *Apogastrostyla rigescens* (Kahl, 1932) gen. nov., comb. nov. (Ciliophora, Hypotricha): morphology, notes on cell division, SSU rRNA gene sequence data, and neotypification. Acta Protozoologica, 49:195-212.

Lynn DH, 2008. The ciliated protozoa: characterization, classification, and guide to the literature. 3rd ed. Pergamon Press, New York, pp. 1-605.

Posada D, 2008. JModelTest: phylogenetic model averaging. Molecular Biology and Evolution, 25:1253-1256. https://doi.org/10.1093/molbev/msn083

Ronquist F, Huelsenbeck JP, 2003. MrBayes 3: Bayesian phylogenetic inference under mixed models. Bioinformatics, 19: 1572-1574. https://doi.org/10.1093/bioinformatics/btg180

Shao C, Lv Z, Pan Y, Al-Rasheid KAS, Yi Z, 2014. Morphology and phylogenetic analysis of two oxytrichid soil ciliates from China, *Oxytricha paragranulifera* n. sp. and *Oxytricha granulifera* Foissner and Adam, 1983 (Protista, Ciliophora, Hypotrichia). International Journal of Systematic and Evolutionary Microbiology, 64:3016-3027. https://doi.org/10.1099/ijs.0.062281-0

Shazib SUA, Vd'ačný P, Kim JH, Jang SW, Shin MK, 2014. Phylogenetic relationships of the ciliate class Heterotrichea (Protista, Ciliophora, Postciliodesmatophora) inferred from multiple molecular markers and multifaceted analysis strategy. Molecular Phylogenetics and Evolution, 78:118-135. https://doi.org/10.1016/j.ympev.2014.05.012

Shi X, Wei H, Wang C, 1997. Morphology studies on a new species of *Oxytricha*, *Oxytricha* shii sp. nov. (Ciliophora: Hypotrichida: Oxytrichidae). Acta Zootaxonomica Sinica, 22:225-230.

Singh J, Kamra K, Sapra GR, 2013. Morphology, ontogenesis, and molecular phylogeny of an Indian population of *Cyrtohymena* (*Cyrtohymenides*) *shii*, including remarks on the subgenus. European Journal of Protistology, 49:283-297. https://doi.org/10.1016/j.ejop.2012.08.009

Talavera G, Castresana J, 2007. Improvement of phylogenies after removing divergent and ambiguously aligned blocks from protein sequence alignments. Systematic Biology, 56:564-577. https://doi.org/10.1080/10635150701472164

Tamura K, Stecher G, Peterson D, Filipski A, Kumar S, 2013. MEGA6: Molecular evolutionary genetics analysis version 6.0. Molecular Biology and Evolution, 30:2725-2729. https://doi.org/10.1093/molbev/mst197

Tsai SF, Chen WT, Chiang KP, 2015. Phylogenetic position of the genus *Cyrtostrombidium*, with a description of *Cyrtostrombidium paralongisomum* nov. spec. and a redescription of *Cyrtostrombidium longisomum* Lynn & Gilron, 1993 (Protozoa, Ciliophora) based on live observation, protargol impregnation, and 18S rDNA sequences. Journal of Eukaryotic Microbiology, 62:239-248. https://doi.org/10.1111/jeu.12173

Wang R, Qiu Z, Chen J, Warren A, Song W, 2007. Morphogenesis of the freshwater ciliate *Neokeronopsis spectabilis* (Kahl 1932) Warren et al., 2002, based on a China population (Ciliophora: Urostylidae). Journal of Eukaryotic Microbiology, 54:184-190. https://doi.org/10.1111/j.1550-7408.2007.00248.x

Warren A, Fyda J, Song W, 2002. The morphology of the poorly-known freshwater urostylid ciliate *Neokeronopsis spectabilis* (Kahl, 1932) nov. gen., nov. comb., (Ciliophora: Urostylidae), with notes on its morphogenesis. European Journal of Protistology, 38:195-206. https://doi.org/10.1078/0932-4739-00820

Wilbert N, 1975. Eine verbesserte Technik der protargolimprägnation für Ciliatenm. Mikrokosmos, 64:171-179.

Received July 16, 2017
Revised January 16, 2018
Accepted January 18, 2018